2015 International Symposium on Nonlinear Theory and its Applications
NOLTA2015, Kowloon, Hong Kong, China, December 1-4, 2015

# Scaling Parameters and Chaos in Generalized 1D Discrete Time Maps

Wafaa S. Sayed†, Ahmed G. Radwan†*, Hossam A. H. Fahmy‡, and Abdel-Latif E. Hussien†

†Engineering Mathematics and Physics Department, Faculty of Engineering, Cairo University, Giza, Egypt 12613
* Nanoelectronics Integrated Systems Center, Nile University, Cairo, Egypt 12588
‡Electronics and Electrical Communications Department, Faculty of Engineering, Cairo University, Giza, Egypt 12613
Email: wafaa.s.sayed@eng.cu.edu.eg, agradwan@ieee.org, hfahmy@alumni.stanford.edu

**Abstract**—Among all chaotic generators, 1D discrete maps are characterized by their simplicity and suitability for digital implementation, in addition to their widely spread applications. Generalizations on 1D discrete maps enhance their unpredictability and increase their reliability in secure communication and encryption. In this paper, three parameterized maps are discussed: scaled positive logistic map (SPLM), scaled mostly positive logistic map (SMPLM), and scaled tent map (STM). The impacts of the introduced scaling parameters on the properties of each map are discussed including: the bifurcation diagram versus the main system parameter, the main keypoints, the maximum chaotic range, and calculation of maximum Lyapunov exponent (MLE) versus all system parameters.

## 1. Introduction

Chaos, first defined by Lorenz [1], is identified with non-periodicity and sensitive dependence on initial conditions and characterized by its complicated dynamics. Chaotic generators, especially 1D maps, are employed in many fields such as: biology, chemistry, physics [2], encryption [3, 4], finance, and others. This explains the need for their analog and digital realizations [5–8]. Early contributions on 1D discrete chaotic maps are owed to May [9] and Feigenbaum [10]. Simple iterative relations may exhibit chaotic behavior for some ranges of the involved parameters. Some of these relations are non-linear, e.g., the logistic map (LM) [2] given by

$$x_{n+1} = f(x_n, \lambda) = \lambda x_n(1 - x_n),\ \lambda \in [0, 4],\ x_n \in [0, 1], \quad (1)$$

and the recently proposed mostly positive logistic map (MPLM) [11] given by

$$x_{n+1} = f(x_n, r) = -r x_n(1 - x_n),\ r \in [0, 2],\ x_n \in [-0.5, 1.5], \quad (2)$$

while others are piece-wise linear such as the tent map (TM) [2] given by

$$x_{n+1} = f(x_n, \mu) = \mu \min(x_n, 1 - x_n),\ \mu \in [0, 2],\ x_n \in [0, 1], \quad (3)$$

where $x_n$ is the iterated variable, while $\lambda$, $r$, and $\mu$ are the system parameters for each map respectively. Bifurcation appears in the form of change of the type of steady state solution versus parameter; from fixed point, followed by a period doubling, quadrupling, etc., that accompanies the onset of chaos. Figure 1 shows the bifurcation diagrams of the three maps previously defined. Since chaos also represents rapid divergence of nearby points, a quantity that measures the rate of this divergence would be quite useful. Theoretically, chaotic behavior is associated with a positive value for the maximum Lyapunov exponent (MLE) [2] given by

$$\text{MLE} = \lim_{n\to\infty}\left(\frac{1}{n}\sum_{i=0}^{n-1}\ln|f'(x_i)|\right), \quad (4)$$

where ln is the natural logarithm. For TM, the maximum chaotic behavior is recorded at $\mu_{max} = 2$ with MLE $= \ln 2$. This value could be proved for TM and by conjugacy for LM at $\lambda_{max} = 4$ [2], similarly for MPLM at $r_{max} = 2$. Figure 1 indicates this value for the three maps. The rest of

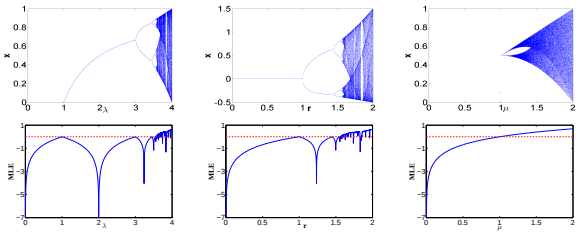

(a) (b) (c)

Figure 1: Bifurcation diagram and MLE versus $\lambda$, $r$, and $\mu$ for (a) LM, (b) MPLM, and (c) TM respectively

this paper discusses the properties of three generalized versions of the previously defined maps employing scaling parameters. Three sections are devoted to the scaled positive logistic map (SPLM), scaled mostly positive logistic map (SMPLM), and scaled tent map (STM) respectively. For each map, the allowed ranges of parameters, fixed points and their stability, and MLE versus all the parameters of the generalized map are discussed. The impacts of the added scaling parameters on multiple properties of each map are studied emphasizing on maximum chaotic response. These properties include: the value of the main system parameter at which maximum chaos occurs, the corresponding output range, and the calculated MLE. The last section concludes the main contributions of the paper.

## 2. Scaled Positive Logistic Map (SPLM)

In this map, two parameters $a$ and $b$ are added to allow scaling both horizontal and vertical axes of the bifurcation diagram and getting different system responses w.r.t. each parameter according to [11]. The map is given by

$$f(x, \lambda, a, b) = \lambda x(a - bx), \qquad \lambda,\ a,\ b \in R^{+}, \tag{5}$$

and is plotted as shown in Fig. 2(a).

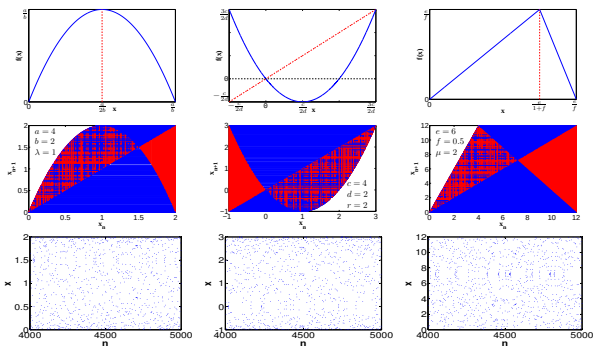

(a) (b) (c)

Figure 2: Function plot, cobweb diagram, and time waveform of chaotic (a) SPLM, (b) SMPLM, and (c) STM

### 2.1. Range of $\lambda$

The roots of the map, its critical point $x_c$, and its maximum value $x_{max}$ are given by:

$$f(x) = 0 \text{ for } x = 0,\ \frac{a}{b}, \tag{6a}$$

$$x_c = \frac{a}{2b},\ f(x_c, \lambda_{max}, a, b) = \frac{a^2\lambda_{max}}{4b} \leq \frac{a}{b} \rightarrow \lambda_{max} \leq \frac{4}{a}. \tag{6b}$$

This inequality not only provides us with information on the maximum value of the parameter $\lambda$, but also that of the parameter $a$. Therefore, the maximum values for the parameters of the map are:

$$(\lambda_{max}, x_{max}) = \left(\frac{4}{a}, \frac{a}{b}\right), \tag{7a}$$

$$a \in (0, a_{max}] \text{ where } a_{max} = \frac{4}{\lambda}, \tag{7b}$$

where confining $x$ to the interval $x \in [0, a/b]$ ensures bounded output for all iterations. Figure 2(a) shows the cobweb diagram and time waveform at $\lambda_{max}$ indicating chaotic behavior in the full range.

### 2.2. Fixed Points and Stability Condition

The fixed points are given by $x^* = f(x^*, \lambda, a, b)$, then

$$x_1{}^* = 0 \text{ and } x_2{}^* = \frac{1}{b}\left(a - \frac{1}{\lambda}\right). \tag{8}$$

The absolute value of the first derivative w.r.t. $x$ at the fixed points determines whether they are stable or unstable when it is less or greater than "one" respectively. Otherwise, if the absolute value equals "one", then it is called a bifurcation point. Therefore, the values of $\lambda$ at which the system bifurcates and their corresponding function values are

$$(\lambda_b, x_b) = \left\{\left(\frac{1}{a}, 0\right), \left(\frac{3}{a}, \frac{2a}{3b}\right)\right\}. \tag{9}$$

Figures 3(a) and (b) show snapshots of the bifurcation diagrams versus the main parameter $\lambda$ at different values of $a$ while $b$ is fixed, and different values of $b$ while $a$ is fixed respectively. The diagrams indicate that the value of $\lambda_{max}$ depends on the parameter $a$ only irrespective of $b$, while both parameters have an impact on the output range which is consistent with the previous analysis. The same results could be derived in another way using the substitution $x_n = (a/b)y_n$ in the iterative relation corresponding to (5) that yields a map quite similar to LM except that its parameter equals $\lambda a$ instead of $\lambda$. Thus, the output of SPLM is $(a/b)$ times that of LM and its parameter is $(1/a)$ times that of LM.

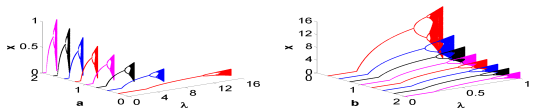

(a) (b)

Figure 3: Bifurcation diagram vs. $\lambda$ for SPLM at (a) $b = 2$ and $a = \{0.25, 0.5, \ldots, 2\}$ and (b) $a = 4$ and $b = \{0.25, 0.5, \ldots, 2\}$

### 2.3. Maximum Lyapunov Exponent

Figure 4(a) shows 3D plot of MLE as a function of both $\lambda$ and $a$ at $b = 2$ for SPLM. It illustrates the dependence of the allowed range of $\lambda$ on the value of $a$ according to equation (7a) where $\lambda_{max}$ is independent of $b$. The parameter $b$ has no impact on the range of the main system parameter as shown in Fig. 4(b). However, the value of MLE approaches the same steady state value of $\ln 2$ for maximum chaotic behavior, or at $\lambda_{max}$. Figure 4(c) shows the values of MLE at $\lambda_{max}$ in the $a-b$ plane indicating that setting the main system parameter to $\lambda_{max}$ corresponding to $a$ achieves maximum chaotic behavior irrespective of $b$. It could be proved using the substitution defined in the previous subsection and the chain rule of derivatives that MLE of SPLM is the same as that of LM with parameter $\lambda a$ instead of $\lambda$. A similar proof could be conducted for SMPLM. Figure 4(d) shows the maximum chaotic output in the $a - b$ plane where generally the lower and upper bounds on the range are constrained by the values of $a$ and $b$ according to equation (7a). In order to get a wider output range, we could increase $a$ and/or decrease $b$.

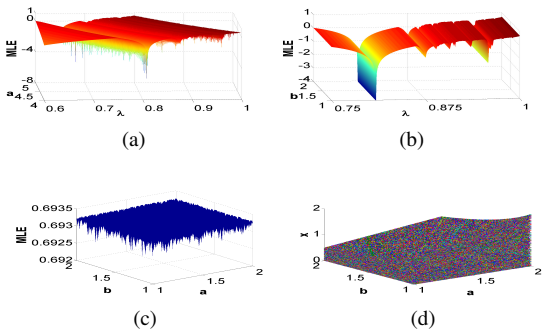


(a) (b) (c) (d)

Figure 4: MLE of SPLM as a function of (a) $\lambda$ and $a$ at $b = 2$, (b) $\lambda$ and $b$ at $a = 4$, (c) $a$ and $b$ at $\lambda_{max}$, and (d) Full-range chaotic output versus $a$ and $b$

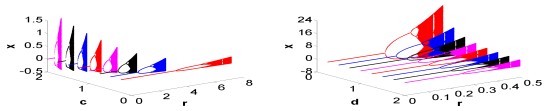


(a) (b)

Figure 5: Bifurcation diagram vs. $r$ for SMPLM at (a) $d = 2$ and $c = \{0.25, 0.5, \ldots, 2\}$ and (b) $c = 4$ and $d = \{0.25, 0.5, \ldots, 2\}$

## 3. Scaled Mostly Positive Logistic Map (SMPLM)

The mostly positive logistic map has been proposed in [11] analyzing its properties in unity scaling case, and extending the analysis to a scaled version utilizing two parameters $c$ and $d$. The general equation of SMPLM is given by

$$f(x, r, c, d) = -rx(c - dx), \qquad r,\ c,\ d \in R^{+}. \tag{10}$$

Its properties could be derived similar to SPLM where

$$(r_{max}, x_{min}, x_{max}) = \left(\frac{2}{c}, -\frac{c}{2d}, \frac{3c}{2d}\right), \tag{11a}$$

$$c \in (0, c_{max}] \text{ where } c_{max} = \frac{2}{r}, \tag{11b}$$

$$(r_b, x_b) = \left(\frac{1}{c}, 0\right). \tag{12}$$

Figure 2(b) indicates that the map exhibits full range chaotic behavior at $r_{max}$. Figure 5 shows that the dependence of the SMPLM on the parameters $c$ and $d$ could be described in a similar way to that of SPLM on the parameters $a$ and $b$ respectively. Figure 6 shows the impact of both $c$ and $d$ on MLE and chaotic output that could be described similar to SPLM.

## 4. Scaled Tent Map (STM)

The scaled tent map proposed in [12] preserves the linearity of the two intersecting lines providing the possibility

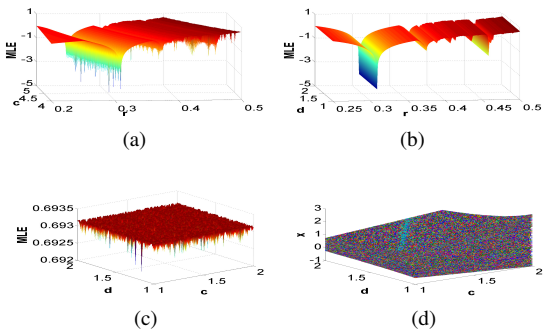


(a) (b) (c) (d)

Figure 6: MLE of SMPLM as a function of (a) $r$ and $c$ at $d = 2$, (b) $r$ and $d$ at $c = 4$, (c) $c$ and $d$ at $r_{max}$, and (d) Full-range chaotic output versus $c$ and $d$

of designing an asymmetric scalable tent shape.

$$f(x, \mu, e, f) = \mu min(x, e - fx), \qquad \mu,\ e,\ f \in R^{+}, \tag{13a}$$

$$f(x, \mu, e, f) = \begin{cases} \mu x & x \le x_k \\ \mu(e - fx) & x_k < x \end{cases}, \ x_k = \frac{e}{1 + f}. \tag{13b}$$

### 4.1. Ranges, Fixed Points, and Stability Condition

The solution should belong to the interval $x \in [0, e/f]$ to guarantee boundedness.

$$(\mu_{max}, x_{max}) = \left(1 + \frac{1}{f}, \frac{e}{f}\right), \tag{14a}$$

$$f \in (0, f_{max}] \text{ where } f_{max} = \frac{1}{\mu - 1}. \tag{14b}$$

Figure 2(c) shows full chaos at $\mu_{max}$. The fixed points are given by

$$x_1^* = 0 \text{ and } x_2^* = \frac{e\mu}{1 + f\mu}. \tag{15}$$

The value of $\mu$ at which the system bifurcates and the region of trivial fixed point ends, in addition to its corresponding function value is

$$(\mu_{b1}, x_{b1}) = (1, 0). \tag{16}$$

For $0 < f < 1$, a region of non-trivial fixed point appears after which the response bifurcates to a period-2 solution given by

$$(\mu_{b2}, x_{b2}) = \left(\frac{1}{f}, \frac{e}{2f}\right). \tag{17}$$

Figure 7 shows that the impact of parameters is reversed in the case of STM compared to logistic map(s). The value of $\mu_{max}$ depends only on the parameter $f$.

### 4.2. Maximum Lyapunov Exponent

Unlike logistic map(s), the allowed range of $\mu$ depends on the parameter $f$ only irrespective of $e$. The largest value for MLE at $\mu_{max}$ in the $e - f$ plane is obtained at $f = 1$

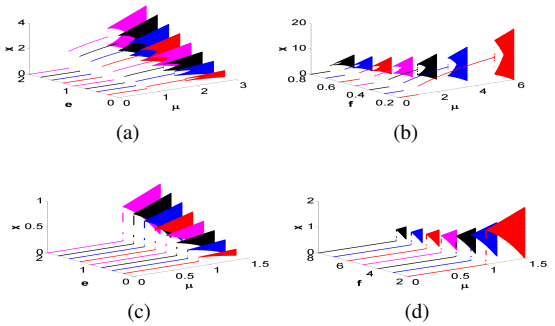

(a) (b) (c) (d)

Figure 7: Bifurcation diagram vs. $\mu$ for STM at (a) $f = 0.5$ and $e = \{0.25, 0.5, \ldots, 2\}$, (b) $e = 4$ and $f = \{0.2, 0.3, \ldots, 0.8\}$, (c) $f = 2$ and $e = \{0.25, 0.5, \ldots, 2\}$, and (d) $e = 4$ and $f = \{2, 3, \ldots, 8\}$

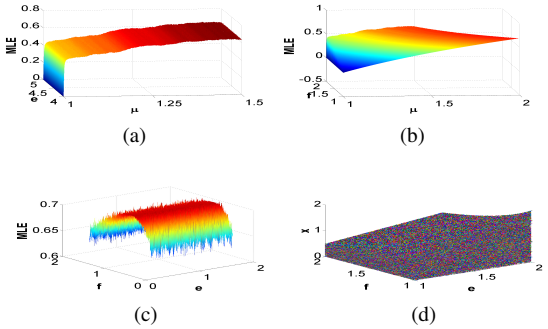

(a) (b) (c) (d)

Figure 8: MLE of STM as a function of (a) $\mu$ and $e$ at $f = 2$, (b) $\mu$ and $f$ at $e = 4$, (c) $e$ and $f$ at $\mu_{max}$, and (d) Full-range chaotic output versus $e$ and $f$

($\mu_{max} = 2$) irrespective of the value of $e$, and equals $\ln 2$. Although this value slightly decreases for other values of $f$, it is still within the same positive range indicating chaotic behavior. Yet, the full range at maximum chaos depends on $e/f$ similar to logistic map(s) as shown in Fig. 8.

## 5. Conclusion

The impact of scaling parameters on the properties of three generalized maps has been studied. In each map, a term in the form of $(m - nx)$ appears where $m$ and $n$ are the scaling parameters. The lower and upper bounds on the output range of each map are scaled by $m/n$. Thus, the maximum output range could be controlled through adjusting their values. For scaled positive and mostly positive logistic maps, the value of the system parameter at which maximum chaotic behavior or full output range is achieved depends on the value of $m$. On the other hand, for scaled tent map it depends on the parameter $n$. In both cases, the main system parameter and the scaling parameter are inversely related. Maximum Lyapunov exponent and chaotic outputs in the $m-n$ plane have been calculated. The results show that the maps exhibit controllable chaotic behavior that could be adapted using the introduced parameters to fit requirements of various applications.

## References


[1] E. N. Lorenz. Deterministic nonperiodic flow. *Journal of the atmospheric sciences*, 20(2):130–141, 1963.

[2] S. H. Strogatz. *Nonlinear dynamics and chaos: with applications to physics, biology, chemistry, and engineering*. Westview press, 2014.

[3] A. G. Radwan, S. K. Abd-El-Hafiz, and S. H. AbdElHaleem. An image encryption system based on generalized discrete maps. In *IEEE International Conference on Electronics, Circuits and Systems (ICECS), 21st*, pages 283–286. IEEE, 2014.

[4] S. K. Abd-El-Hafiz, A. G. Radwan, and S. H. AbdElHaleem. Encryption applications of a generalized chaotic map. *Appl. Math. Inf. Sci.*, 9(6):1–19, 2015.

[5] A. G. Radwan, A. M. Soliman, and A. El-Sedeek. MOS realization of the modified lorenz chaotic system. *Chaos, Solitons & Fractals*, 21(3):553–561, 2004.

[6] A. G. Radwan, A. M. Soliman, and A. S. Elwakil. 1-D digitally-controlled multiscroll chaos generator. *International Journal of Bifurcation and Chaos*, 17(01):227–242, 2007.

[7] M. L. Barakat, A. G. Radwan, and K. N. Salama. Hardware realization of chaos based block cipher for image encryption. In *ICM, 2011*, pages 1–5. IEEE, 2011.

[8] M. A. Zidan, A. G. Radwan, and K. N. Salama. Controllable V-shape multiscroll butterfly attractor: system and circuit implementation. *International Journal of Bifurcation and Chaos*, 22(06), 2012.

[9] R. M. May et al. Simple mathematical models with very complicated dynamics. *Nature*, 261(5560):459–467, 1976.

[10] M. J. Feigenbaum. Quantitative universality for a class of nonlinear transformations. *Journal of statistical physics*, 19(1):25–52, 1978.

[11] W. S. Sayed, A. G. Radwan, and H. A. H. Fahmy. Design of positive, negative, and alternating sign generalized logistic maps. *Discrete Dynamics in Nature and Society*. Article ID 586783, 2015.

[12] A. G. Radwan and S. K. Abd-El-Hafiz. Image encryption using generalized tent map. In *IEEE 20th International Conference on Electronics, Circuits, and Systems (ICECS)*, pages 653–656. IEEE, 2013.